Macromolecules

pubs.acs.org/Macromolecules Article

Importance of Nucleophilicity of Chain-Transfer Agents for Controlled Cationic Degenerative Chain-Transfer Polymerization

Parker Thomas Boeck, Joji Tanaka,* Shubin Liu, and Wei You*

Cite This: *Macromolecules* 2020, 53, 4303−4311 Read Online

ACCESS | Metrics & More | Article Recommendations | Supporting Information

ABSTRACT: Research on controlling cationic polymerization through a degenerative chain-transfer (DCT) process has primarily focused on the family of vinyl ether monomers. To expand the monomer scope, a better understanding on what properties of chain-transfer agents (CTA)s to achieve satisfactory cationic DCT is necessary. In this work, we focused on *para*-methoxystyrene (*p*MOS) as the model monomer for electron-rich styrenics and screened a library of CTAs varying in acidity and nucleophilicity. Our results showed that increasing the nucleophilicity of the CTAs significantly improved the control over the cationic DCT polymerization of *p*MOS. In contrast, acidic CTAs, which provide good control over the cationic DCT polymerization of vinyl ethers, do not exert appreciable control of the cationic DCT polymerization of *p*MOS. Furthermore, we discovered two new CTAs for controlling the cationic DCT polymerization of *p*MOS, 1-butaneselenol and benzeneselenol. Lastly, this systematic study allowed us to develop a hypothesis about how the electronic structure of the propagating carbocation dictates the characteristics of a CTA necessary to control the cationic DCT polymerization of a given monomer.

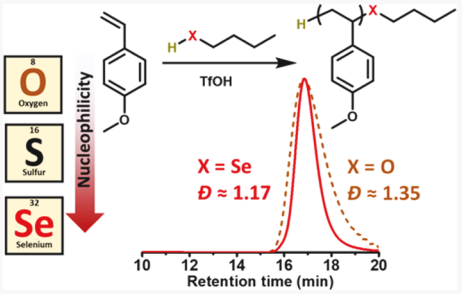

1. INTRODUCTION

Studies on controlled chain-growth polymerizations have strayed away from ionic-centered living polymerizations (i.e., anionic and cationic)[1−3] since the dawn of reversible-deactivation-radical polymerization methodologies that are radical-centered.[4−7] However, a resurgence in cationic-centered polymerization has recently occurred.[8] Typically, cationic polymerization has been largely limited to electron-rich vinyl monomers such as vinyl ethers (VEs) and *para*-methoxystyrene (*p*MOS) that are difficult to polymerize through a radical-based process.[9,10] To further expand the scope of accessible polymer compositions, recent advancements have enabled copolymerizations of these monomers with a variety of radical monomers.[11−18] Additionally, the incorporation of renewable feedstock as monomers[19−22] and degradable building blocks have also been made possible through cationic polymerizations.[23−25] Furthermore, the nature of the propagating cation can serve to control the sequence in terpolymerization.[26] More recently, an unprecedented discovery—catalyst-controlled stereoselective cationic polymerization of VEs—has been demonstrated by Teator and Leibfarth,[27,28] where poly(vinyl ether)s of high isotacticity show distinctive physical properties. All these exciting discoveries call for further exploration of cationic polymerizations for precise control over molecular weight and complex architectures.[29,30] To this end, facile and mild alternative protocols for controlling cationic polymerization have emerged.[13,31,32] Of particular note, Fors and co-workers recently demonstrated a single-component system that initiates and controls the cationic polymerization of VEs in the absence of additional controlling agents; impressively, this new system-based cationic polymerization can be conducted at ambient temperature and open to air.[33]

Until recently, living/controlled cationic polymerizations were typically controlled by reversible activation of a dormant carbon−halogen bond to reactive carbocationic species via metal-based Lewis acid catalysts.[34] However, building upon the discovery of using isobutyl VE (IBVE)−thiocarbonylthio/dithiocarbamate adducts to cross over from a RAFT (reversible addition−fragmentation chain transfer)-mediated radical polymerization to a living cationic polymerization upon activation by a Lewis acid,[16,35] Kamigaito and co-workers reported the RAFT-based degenerative chain-transfer (DCT) control of the cationic polymerization of VEs, *p*MOS, and *p*-hydroxystyrene, externally initiated by a strong Brønsted acid (trifluoromethanesulfonic acid, TfOH), demonstrating the first controlled cationic RAFT polymerization (Scheme 1D).[36] This discovery represented a significant advancement over the original living cationic polymerization, because the chemical nature of the chain-transfer agent (CTA) can now modulate the control over cationic chain transfer, similar to radical-centered RAFT polymerization. Therefore, in principle, one could engineer

Received: February 5, 2020
Revised: April 21, 2020
Published: May 20, 2020

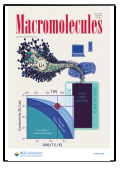

https://dx.doi.org/10.1021/acs.macromol.0c00290
Macromolecules 2020, 53, 4303−4311

Scheme 1. Mechanism of DCT-Controlled Cationic Polymerization (A) Mechanism, (B) Monomers, and (C) CTAs Investigated in This Work; (D) Comparison with RAFT-Controlled Cationic Polymerization

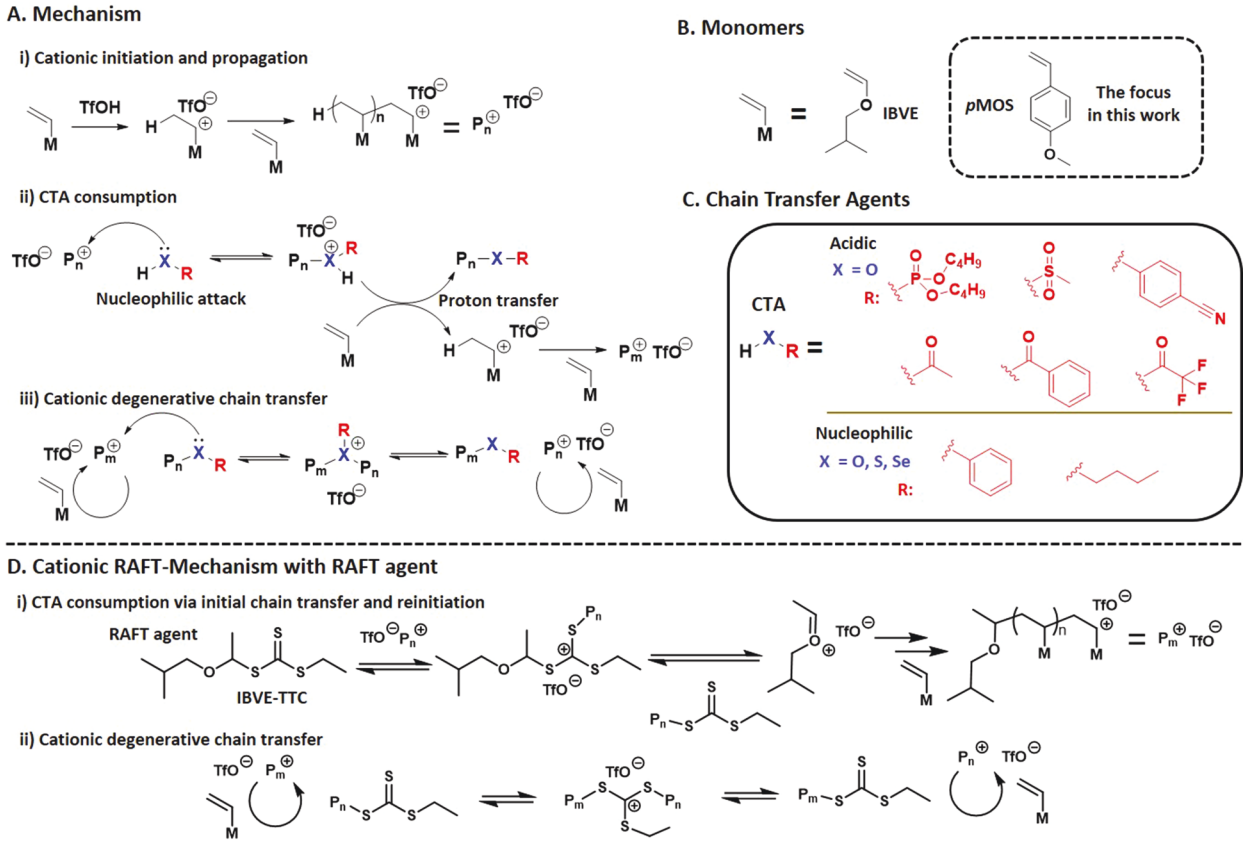

the structure of the CTA to make cationic RAFT polymerization amenable to a wider scope of monomers beyond the reported monomers. Straying away from acidic initiators, Kottisch *et al.* reported the photocontrolled cationic polymerization of VEs using dithiocarbamate- and trithiocarbonate-based CTAs with an oxidizing photocatalyst.[17,18] Unfortunately, despite the establishment of multiple living cationic polymerization techniques, their scope of the monomers remains limited primarily to VEs. User-friendly approaches to the controlled cationic polymerization of electron-rich styrenics, for example, *p*MOS, are underrepresented. In an effort to fill this void, Prasher *et al.* reported the controlled cationic polymerization of *p*MOS using methanol as the CTA and TfOH as the initiator,[10] confirming the cationic DCT-controlled polymerization of *p*MOS with methanol as the CTA with a photoredox catalyst, first reported by Perkowski *et al.*[37]

Whereas *p*MOS and VEs are both electron-rich vinyl monomers, they have significantly different electronic structures, which dictate their reactivity, rate of polymerization, and efficiency of chain transfer. For example, Uchiyama *et al.* reported that the polymerization of IBVE took 1 min to reach 93% monomer conversion; yet, with the same CTA (i.e., thiophenol−IBVE adduct), *p*MOS took 14 h to reach 97% monomer conversion.[38] This phenomenon can be explained by the fact that the propagating carbocation center of VEs is significantly less stable, as there is only an oxygen that can donate electron density to stabilize the cation.[39] On the other hand, the propagating carbocation of *p*MOS is stabilized through resonance donation of electron density by the aromatic ring and the oxygen on the 4-position of the ring. Thus, the propagating carbocation of *p*MOS is significantly more stable than that of VEs (e.g., IBVE), resulting in inherently slower propagation. Despite this reasonable explanation, little has been done to experimentally establish a relationship between the electronic structure of the propagating carbocation and its impact on the characteristics needed in a CTA.

For the cationic DCT polymerization of VEs, Uchiyama *et al.* recently screened a variety of CTAs.[9] Of those CTAs, dibutyl phosphate (*n*-BuO_2PO_2H) provided excellent control over the molecular weight, accompanied by narrow molecular weight distributions, whereas methanesulfonic acid (CH_3SO_3H) provided only moderate control. However, no such screening has been done for electron-rich styrenics (e.g., *p*MOS). Therefore, to understand how different CTAs would affect the cationic polymerization of electronic-rich styrenics (rate, dispersity, molecular weight evolution, etc.), we screened a library of nucleophilic and acidic CTAs' ability to control the cationic polymerization of *p*MOS. Our results indicate that, the difference in effective CTAs between *p*MOS and VEs (e.g., IBVE) can be explained by the difference in the stability of the propagating carbocations. Furthermore, we demonstrate that increasing the nucleophilicity of the CTA improves the control in the cationic DCT polymerization of *p*MOS. Finally, we discover two novel selenium-based CTAs, butaneselenol and selenobenzene, that provide superior control over the cationic polymerization of *p*MOS when compared with analogous sulfur and oxygen-based CTAs.

https://dx.doi.org/10.1021/acs.macromol.0c00290
Macromolecules 2020, 53, 4303−4311

2. EXPERIMENTAL SECTION

2.1. Materials. Anhydrous solvents were collected from a glass contour solvent system purchased from Pure Process Technology LLC and stored over 4 Å molecular sieves. *p*MOS was distilled over calcium hydride under reduced pressure. The TfOH stock solution (20 mg/mL) was prepared in a glovebox because of its hydroscopic nature with anhydrous diethyl ether. All other reagents were purchased from Sigma-Aldrich Corporation, VWR International, and Fisher Scientific Corporation and used without additional purification unless otherwise noted.

2.2. Instrumentations. ^{1}H NMR spectra were recorded on a Bruker DRX 400 MHz spectrometer using a solvent residual peak as the internal standard (at 7.26 ppm in $CDCl_3$). Size exclusion chromatography (SEC) was performed on a Waters 2695 separations module liquid chromatograph equipped with two Agilent Resipore columns (PL1113-6300) maintained at 35 °C, and a Waters 2412 refractive index detector at room temperature. Tetrahydrofuran (THF) was used as the mobile phase at a flow rate of 1.0 mL/min. Molar mass and dispersity data are reported relative to 580−200,000 g/mol poly(styrene) standards. Matrix-assisted laser desorption/ionization-time of flight-mass spectrometry (MALDI-ToF-MS) spectra were recorded using an AB Sciex 5800 MALDI-ToF/ToF in reflector mode with a voltage multiplier of 0.66 and 3550 laser intensity.

2.3. Polymerization Procedures. In a typical polymerization, a monomer (*p*MOS, 495.5 μL 500 mg, 3.73 mmol), a solvent (anhydrous dichloromethane, 6.82 mL), and CTA (butanol, 13.64 μL, 11.04 mg, 0.149 mmol) were added to a scintillation vial containing a magnetic stirrer. This solution was cooled to 0 °C with stirring. Then, TfOH prepared as a 20 mg/mL stock solution in diethyl ether was added (0.139 mL, 2.79 mg, 0.0186 mmol) to initiate the polymerization. After an hour and a half, reactions were quenched with excess triethylamine. To confirm monomer conversion, an aliquot of the reaction mixture was analyzed by ^{1}H NMR analysis. The polymer was then isolated by precipitation into methanol for further analysis. Experimental number average molar mass ($M_{n,sec}$) and dispersity ($Đ$) were determined by SEC analysis.

For kinetic studies, 0.4 mL aliquots were removed at regular intervals and added to THF (for SEC analysis) and deuterated chloroform (for ^{1}H NMR analysis) containing triethylamine to prevent further propagation. Monomer conversion was calculated using ^{1}H NMR by integrating the −CH*H* vinylic proton at 5.6 ppm and using the −OCH_3 phenyl-methoxy proton at 3.80 ppm as an internal reference. Experimental number average molar mass ($M_{n,sec}$) and dispersity ($Đ$) were determined by SEC analysis.

For in situ chain extension, conversion was confirmed by ^{1}H NMR and an equivalent amount of monomer (*p*MOS, 495.5 μL 500 mg, 3.73 mmol) was added to the reaction mixture. After an hour and a half, full conversion was confirmed by ^{1}H NMR.

2.4. Synthesis of 1-Butaneselenol. Elemental selenium (1.58 g, 20.0 mmol) was added to a dry flask containing a stir bar. The flask

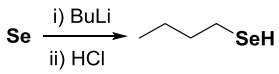

was sealed, and 20 mL of anhydrous THF was added. The solution was then purged with argon for 10 min. Next, the flask was cooled to 0 °C and 8 mL of 2.5 M *n*-butyllithium (1.28 g, 20.0 mmol) in hexanes was added. The flask was allowed to stir at 0 °C for 15 min. The flask was then cooled to −78 °C and 10 mL of 2.0 M hydrochloric acid (20 mmol) was added. The flask was allowed to stir for 15 min at −78 °C and then warmed to room temperature. Salts precipitated upon warming and were filtered off. The solvent was removed under reduced pressure. The product was filtered through silica to remove any residual salts. The final product was a bright yellow liquid with a foul odor. The product was stored under argon to prevent oxidation. Spectroscopic data were consistent with the reported literature values.[40]

2.5. Calculation of Theoretical Number-Average Molar Mass, $M_{n,th}$. The theoretical number-average molar mass was calculated with the following equation.

$$M_{n,th} = \frac{p[M]_0 M_M}{[CTA]_0} + M_{CTA} \quad (1)$$

where $[CTA]_0$ and $[M]_0$ are the initial concentrations (mol/L) of the monomer and CTA, respectively. M_M and M_{CTA} are the molar masses (g/mol) of the monomer and CTA, respectively. Finally, p is the monomer conversion as calculated by ^{1}H NMR analysis. Note, this assumes 100% initiation efficiency from CTAs (and intact CTA-derived terminal end groups) and neglects polymer chains derived from TfOH initiation.

2.6. Computational Calculation. The Gibbs free energy change and Hirsch field charges were obtained through computational chemistry. All calculations were performed at the density functional theory (DFT) wB97XD/6-311 + g(d) level of theory with the implicit solvent model of CPCM in dichloromethane taken into consideration. The software used was Gaussian version 16A03.

3. RESULTS AND DISCUSSION

3.1. Weak Acids as CTAs in Cationic Polymerization. Inspired by the excellent control over the cationic polymerization of VEs using weak protonic acids demonstrated by Uchiyama *et al.*,[9] we began our investigation by screening these weak protonic acids as CTAs for the cationic polymerization of *p*MOS. Our results on *p*MOS are summarized in Table 1, together with the data for VE (i.e., IBVE) from Uchiyama *et al.*[9] The data clearly showed that there is a significant difference in the characteristics of a CTA necessary to control the cationic polymerization of IBVE and *p*MOS. For example, phosphoric acid dibutyl ester ($(n\text{-BuO})_2PO_2H$) was able to offer excellent control over the cationic polymerization of IBVE (Table 1),[9,41] yet it was unable to control the cationic polymerization of *p*MOS (Table 1), resulting in a molar mass that was significantly higher than the targeted molar mass ($M_{n,sec}$ = 16,000 vs $M_{n,th}$ = 3600 g mol^{-1}). The high molar mass observed ($M_{n,sec}$), numerically close to the high $M_{n,sec}$ for the cationic polymerization of *p*MOS without any CTA (Table 1), suggested that this particular CTA (phosphoric acid dibutyl ester) was only consumed to a marginal amount, if consumed at all. Likewise, methanesulfonic acid (CH_3SO_3H) was unable to control the polymerization (Table 1) and gave a dispersity even higher than when no CTA was used, despite the moderate control previously reported for IBVE (Table 1). Other acids, including trifluoroacetic acid (CF_3CO_2H, Table 1), benzoic acid ($PhCO_2H$, Table 1), and acetic acid (CH_3CO_2H, Table 1), were unable to control the cationic polymerization of *p*MOS as well. To further demonstrate the lack of control when using weak acids for the cationic polymerization of *p*MOS, we targeted a range of molar masses by changing the [M]/[CTA] ratio using acetic acid (CH_3CO_2H) as the CTA (Table 1). Again, the observed molar mass did not correlate with the targeted molar mass. In summary, the results made it clear that weakly acidic CTAs cannot control the cationic polymerization of *p*MOS. On the other hand, we previously observed simple alcohols (e.g., methanol and ethanol) as CTA provided moderate control over molar mass for *p*MOS (Table 1);[10] in contrast, a complete lack of control was observed for IBVE (Table 1) when 1-octanol was used as the CTA.[9] Finally, reducing the nucleophilicity of ethanol by partial fluorination into trifluoroethanol was detrimental to controlled cationic DCT polymerization of *p*MOS (Table 1).

https://dx.doi.org/10.1021/acs.macromol.0c00290
Macromolecules 2020, 53, 4303−4311

Table 1. DCT-Controlled Cationic Polymerization of IBVE and *p*MOS Using Acidic CTAs

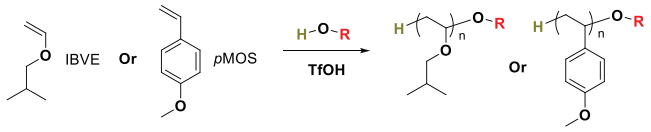

	IBVE[a]			*p*MOS		
CTA	$M_{n,th}$ (g mol^{-1})	$M_{n,sec}$ (g mol^{-1})	$Đ$	$M_{n,th}$[b] (g mol^{-1})	$M_{n,sec}$[c] (g mol^{-1})	$Đ$[c]
$(n\text{-BuO})_2PO_2H$	2500	3100	1.09	3600	16,000	1.48
	5000	5000	1.09			
	10,000	10,500	1.08			
CH_3SO_3H	2500	3000	1.19	3500	20,000	1.98
	4800	5500	1.51			
CF_3CO_2H	4900	17,000	3.36	3500	43,000	3.43
CH_3CO_2H	4800	12,000	2.60	1400	9000	1.39
				3400	9000	1.40
				13,500	18,000	1.50
$PhCO_2H$				3500	16,000	2.39
CH_3OH[d]	5000	3300[d]	1.80[d]	6700	6200[d]	1.22[d]
C_2H_5OH[d]				6700	10,200[d]	1.24[d]
CF_3CH_2OH[d]				6800	26,400[d]	1.71[d]
$n\text{-}C_8H_{17}OH$	5000	11,000	2.83			
C_5H_5OH				3400	12,000	1.34
$p\text{-}CNC_5H_4OH$				3400	27,000	1.68
No CTA		24,600[e]	3.58[e]		21,000	1.67
IBVE-TTC[d]	5000	5000	1.18	6500	5200	1.25

[a]Unless specified, the values are obtained from ref 9. [b]$M_{n,th}$ is the theoretical molar mass calculated from eq 1 (see the Experimental Section). [c]$M_{n,sec}$ is the experimental molar mass determined by SEC in THF with poly(styrene) standards. [d]Reported value from ref 10. [e]Reported value from ref 36.

3.2. Stability of Propagating Cation versus Nucleophilicity of CTAs. The results presented in Table 1 highlight the difference in reactivity of VEs (e.g., IBVE) and styrenics (e.g., *p*MOS) in DCT-controlled cationic polymerization. For example, the nucleophilicity of the monomer is an important factor in the cationic polymerization, as the chain propagation step relies on the reaction between the electrophilic propagating chain end and the nucleophilic monomer. The higher electron density of the β carbon in IBVE compared to *p*MOS greatly promotes the nucleophilic addition of the monomer to the propagating chain end. Furthermore, the propagating cation (i.e., an electrophile) of IBVE is inherently less stable than that of *p*MOS, because of a reduced resonance stabilization of the propagating cationic IBVE species. All these factors contribute to the extremely fast polymerization of IBVE even at a very low temperature (e.g.,−78 °C); in contrast, the cationic polymerization of *p*MOS is much slower even when conducted at a comparably higher temperature (e.g.,−10 °C).

In order to control cationic polymerization via the DCT mechanism (Scheme 1), one would need fast and efficient chain transfer to the CTA to (a) consume CTAs to cap the majority of the chain ends with CTA moieties and (b) establish and maintain the main equilibrium to enable rather uniform chain propagation. Whereas the less-stable and more-reactive propagating cation of IBVE would allow successful chain transfer to less-nucleophilic CTAs, for example, weak acids, we reason that the more-stable cation of *p*MOS would require more nucleophilic CTAs to attack its more stabilized cation-center (Scheme 2).[39] This hypothesis—a less-stable propagating cation being more susceptible to attack by a less-nucleophilic CTA, whereas a more-stable propagating cation requires a more-nucleophilic CTA—can indeed help us understand the cumulative data obtained to date (Table 1). Additionally, the degenerate chain-transfer-controlled cationic polymerization in the presented cases (Scheme 2) would require a proton chain transfer from the initial chain-transfer intermediate to the monomer, in order to complete the consumption of the CTA and initiate new chains (Scheme 2). This proton transfer step would occur much faster with VE because of its higher basicity than *p*MOS, accounting for a higher degree of consumption of CTA and control over the cationic polymerization of VEs. For example, $(n\text{-BuO})_2PO_2H$ and CH_3SO_3H are able to control the cationic polymerization of IBVE, despite being relatively weak nucleophiles; however, neither of these two can exert sufficient control on the cationic polymerization of *p*MOS, given the stable propagating cation of *p*MOS. In contrast, none of the carboxylic acids tested were sufficiently nucleophilic to serve as CTAs for the cationic polymerization of either IBVE or *p*MOS. From our initial screening of CTAs, covering a wide range of acidity (pK_a from ∼0 to ∼5), it became clear that it is the nucleophilicity, rather than the acidity, that exerts the real control over the cationic polymerization of *p*MOS. Furthermore, given that the central element that enables the chain transfer is oxygen (i.e., propagating cation would transfer to the oxygen atom in these acid-based CTAs), one would wonder what might happen to simple alcohols as potential CTAs. Indeed, the data showed that a simple alcohol can sufficiently control the cationic polymerization of *p*MOS (Table 1) but can only offer poor control over the cationic polymerization of IBVE (Table 1). Further decreasing the nucleophilicity from ethanol to trifluoroethanol (CF_3CH_2OH) led to a complete loss of control (Table 1),[10] highlighting the importance of nucleophilicity of the CTA in DCT-controlled cationic polymer-

https://dx.doi.org/10.1021/acs.macromol.0c00290
Macromolecules 2020, 53, 4303−4311

Scheme 2. Representative Resonance Structures of the Propagating Carbocation Center of *p*MOS and IBVE Effecting CTA Consumption in Cationic DCT

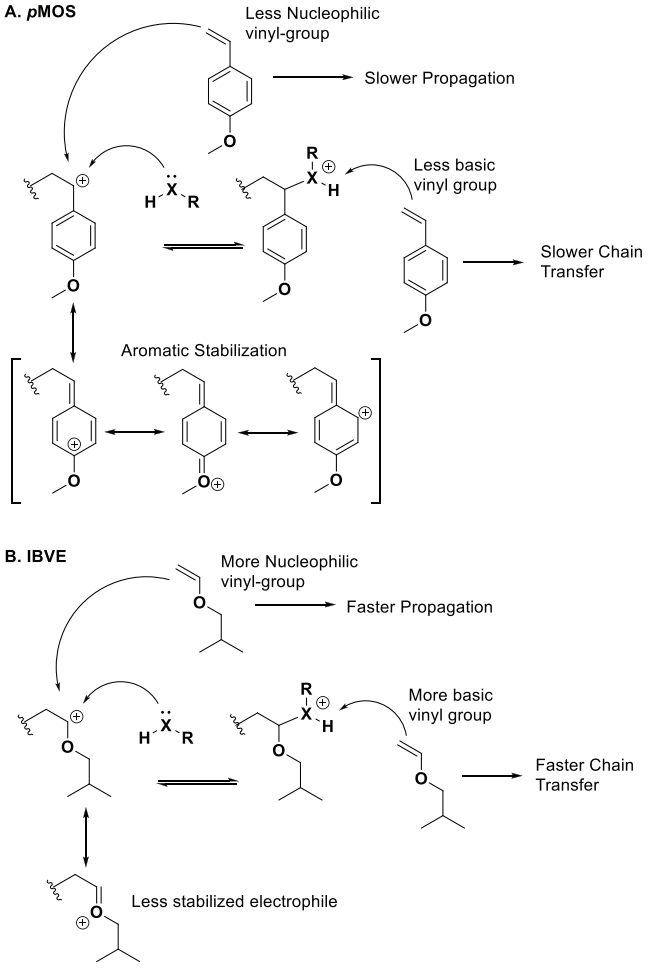

(A) Propagating *p*MOS carbocation is stabilized by aromatic resonance and *p*MOS bares a less basic vinyl group to complete CTA consumption through reinitiation via proton transfer; both factors are unfavorable for efficient CTA consumption; however, slow propagation and low nucleophilicity of the monomer increase the odds of chain-transfer events; (B) propagating carboxonium center of IBVE is comparatively less-stabilized and the vinyl group is more basic, favoring CTA consumption; However, the more-nucleophilic vinyl group is unfavorable for chain-transfer events over propagation.

izations. Consistent with this, mechanistic studies have shown electron-rich or nucleophilic RAFT agents exert better control in photocontrolled cationic RAFT polymerization of VEs.[42]

3.3. Substituted Phenols as CTAs. To further understand the impact of nucleophilicity of the CTA in controlling cationic DCT polymerization, we next investigated a variety of CTAs of varying nucleophilicity in the cationic polymerization of *p*MOS.

We started our investigation with phenol, as the nucleophilicity of the alcohol attached to the benzene can be modulated by using different substituents on the 4-position of the benzene ring. As phenol is significantly less nucleophilic than methanol and would not enable fast chain transfer via nucleophilic attack to the propagating cationic chain end, one would not expect much control over the cationic polymerization of *p*MOS. Indeed, a poor control on the molar mass was observed when phenol was used as the CTA ($M_{n,sec}$ = 12,000 g mol^{-1}, $Đ$ = 1.34) (Figure S1, Table 1), significantly differing from the targeted molar mass ($M_{n,th}$ = 3400 g mol^{-1}). Electronic structure models generated using DFT reveal that there is a significantly higher electron density at the 4-end of the ring (the sp^2 carbon) than at the oxygen (Figure S2). This suggests that nucleophilic addition may occur through a Friedel−Crafts pathway (i.e., more nucleophilic carbon on the 4-position of the phenol attacking the cationic chain end), possibly accounting for the lack of control by phenol as the CTA cationic DCT-controlled polymerization of *p*MOS. Further investigation of these polymers via MALDI-ToF indeed suggests phenol-derived end groups; unfortunately, we could not confirm the structure of the end groups by nuclear magnetic resonance (NMR). Substituting the 4-position of phenol with an electron-withdrawing cyano-group would significantly decrease the electron density on the oxygen, and the reduced nucleophilicity of the oxygen would further lower the ability of the CTA in controlling the cationic polymerization. This was indeed confirmed by the experimental results. Specifically, we observed a much higher molar mass ($M_{n,sec}$ = 27,000 g mol^{-1}) and a broadened dispersity ($Đ$ = 1.68) when using 4-cyanophenol as the CTA (Figure S1, Table 1). Furthermore, computation of the Hirsch field charges confirmed that 4-cyanophenol is significantly less nucleophilic than phenol (i.e., the oxygen as the nucleophile) (Figure S2). These results indicate that decreasing the nucleophilicity of the CTA decreases the ability of the CTA in controlling the cationic polymerization *p*MOS, consistent with our proposed mechanism (Scheme 2).

3.4. Group 16 Aromatic Nucleophiles as CTAs. To confirm the lack of influence over molecular weight control by weakly nucleophilic phenol, we varied the [M]/[CTA] ratio to target a range of degree of polymerizations. Based on our results (Table 2), phenol was unable to control the molecular mass in the cationic polymerization of *p*MOS as varying the [M]/[CTA] did little to change the observed molar mass (Figure S3A). Despite this apparent lack of control, a phenol ω-end capped species was suggested by the MALDI-ToF mass

Table 2. Group 16 Aromatic Nucleophiles-Based CTA-Mediated Cationic Polymerization of pMOS

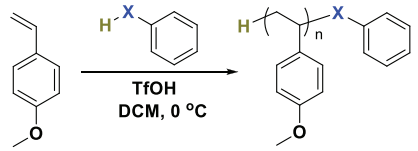

CTA	$M_{n,th}$[a] (g mol^{-1})	$M_{n,sec}$[b] (g mol^{-1})	$Đ$[b]
phenol	1400	7700	1.49
	3400	12,000	1.34
	6700	14,000	1.39
	13,500	14,500	1.39
thiophenol	1400	1000	1.27
	3400	2200	1.51
	6700	5200	1.37
	13,500	11,000	1.45
benzeneselenol	1400	1900	1.17
	3400	3400	1.29
	6700	9400	1.35
	13,500	12,000	1.38

[a]Calculated using eq 1 (see the Experimental Section). [b]Determined by SEC in THF with poly(styrene) standards.

https://dx.doi.org/10.1021/acs.macromol.0c00290
Macromolecules 2020, 53, 4303−4311

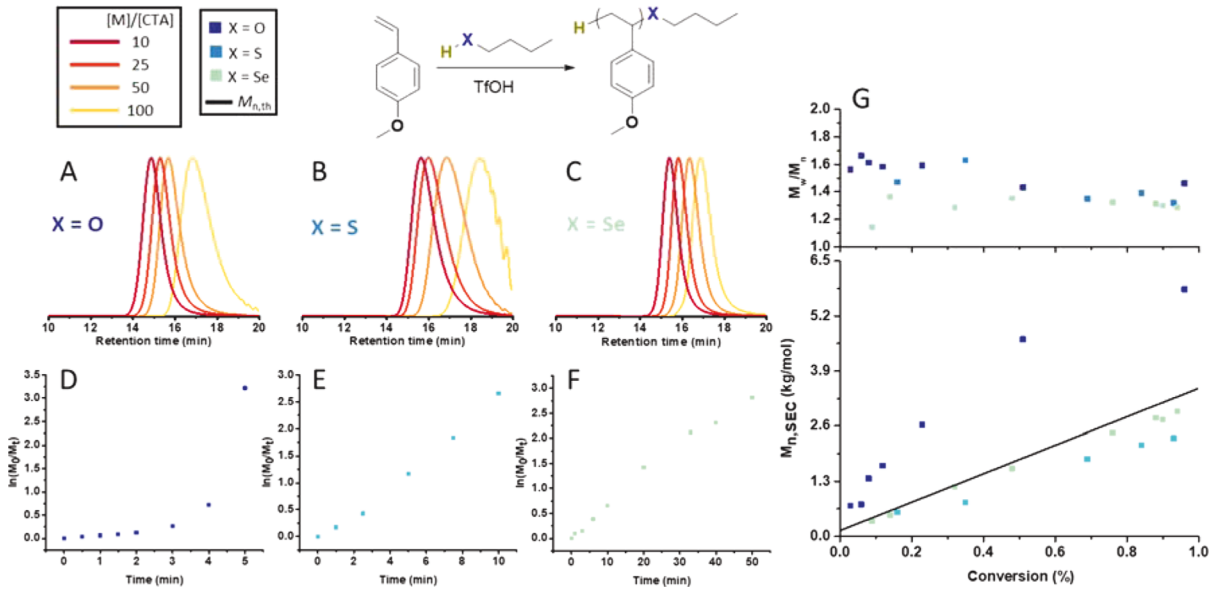

Figure 1. (A–C) Targeting different molar mass of Poly(*p*MOS) and (D–F) kinetic analysis using butanol, butanethiol, and butaneselenol respectively as CTAs for DCT-controlled cationic polymerizations. Molar mass and dispersity evolution with monomer conversion (G).

spectrum (Figure S4), indicating some consumption of the CTA during the polymerization. As a full consumption of the CTA is a prerequisite to achieving excellent control over the polymerization via our proposed mechanism (Scheme 1), we next screened other aromatic nucleophiles from elements in group 16 (e.g., from oxygen to sulfur and selenium), attempting to increase the consumption of the CTA with increased nucleophilicity, and aiming to discover new CTAs that can exert better control on the cationic polymerization of *p*MOS. Pleasingly, changing the nucleophilic component from oxygen (O) to sulfur (S), we observed a dramatic increase in control over the molar mass, likely because of the increased nucleophilicity of sulfur (Figure S3B, Table 2).[43] In contrast to the results in the case of phenol, the observed molar mass was found to be in good agreement with the targeted molar mass (Table 2). Again, a CTA (i.e., thiophenol) ω-capped species was suggested by the MALDI-ToF spectrum (Figure S5). More importantly, with thiophenol as the CTA, we were able to observe both the α-chain end ($-CH_3$, 1.1 ppm) and the ω-chain end ($-SC_6H_5$, 7.1 ppm) by ^{1}H NMR (Figure S6), confirming a significant amount of CTA consumption. In fact, the observed control on the cationic polymerization of *p*MOS by thiophenol was similar to the results observed by Uchiyama *et al*,[38] albeit a thiophenol-*p*MOS monomer adduct-based CTA was used in their case.

Going down group 16 from sulfur (S) to selenium (Se), further increasing CTA softness and nucleophilicity, benzeneselenol was able to exert a similar control on the cationic polymerization of *p*MOS as to when thiophenol was used.[43] Again, by modulating the [M]/[CTA], we were able to target a variety of different molar masses (Figure S3C, Table 2). A benzeneselenol ω-end capped polymer species was also suggested by the MALDI-ToF spectra (Figure S7). Additionally, we observed both the α-chain end ($-CH_3$, 1.0 ppm) and the ω-chain end ($-SeC_6H_5$, 7.25 ppm) by ^{1}H NMR (Figure S8). However, it is important to note that as both sulfur (S) and selenium (Se) can expand their valency (when compared to oxygen), the sulfonium/selenonium intermediate may be further stabilized from the aromatic ring. In addition, cation–π interactions could also affect the polymerization when aromatic CTAs are used.[44] Thus, to deconvolute the effect of nucleophilicity of the CTA from the effect of aromatic resonance stabilization of the sulfonium and selenonium intermediates, we next carried out a series of polymerizations using group 16 aliphatic analogues as CTAs.

3.5. Group 16 Aliphatic Nucleophiles as CTAs. As we discussed earlier, primary alcohols (e.g., ethanol) can provide moderate control over the cationic polymerization of *p*MOS (Table 1). We further verified the capability of primary alcohols in mediating such polymerizations by employing 1-butanol to tune the molar mass based on the [M]/[CTA] ratio (Figure 1A, Table 3). As expected, we were able to identify the α-chain end ($-CH_3$, 1.0 ppm) and the 1-butanol capped ω-chain end ($-OCH_2-$ 3.15 ppm, $-CH_2-$ 1.05, $-CH_2CH_3$ 0.9 ppm) by ^{1}H NMR analysis (Figure S9), corroborated by the observation of the 1-butanol-capped polymer species by the MALDI-ToF MS (Figure S10). When the nucleophilic element was changed from oxygen to sulfur, with the increased

Table 3. Aliphatic Nucleophilic CTA-Controlled Cationic DCT Polymerization of *p*MOS

CTA	$M_{n,th}$[a] (g mol^{-1})	$M_{n,sec}$[b] (g mol^{-1})	$Đ$[b]
1-butanol	1400	2200	1.35
	3400	6200	1.31
	6700	9500	1.29
	13,500	14,400	1.36
1-butanethiol	1400	1000	1.19
	3400	2300	1.34
	6700	4200	1.42
	13,500	5700	1.46
1-butaneselenol	1400	2600	1.17
	3400	3900	1.18
	6700	6900	1.23
	13,500	15,000	1.38

[a]Calculated using eq 1 (see the Experimental Section). [b]Determined by SEC in THF with poly(styrene) standards.

https://dx.doi.org/10.1021/acs.macromol.0c00290
Macromolecules 2020, 53, 4303–4311

CTA nucleophilicity of 1-butanethiol, the observed molar masses were in better agreement with the targeted molar masses (Figure 1B, Table 3).[43] Switching to 1-butaneselenol, the most soft and nucleophilic CTA among this series, we observed the best control over the molar mass of the polymers of *p*MOS (Figure 1C, Table 3).[43] With both 1-butanethiol and 1-butaneselenol, we were able to identify the CTA-capped chain ends via ^{1}H NMR analysis (Figures S11 and S12, respectively), and CTA ω-end capped polymers via MALDI-ToF MS (Figures S13 and S14, respectively). Impressed by the control provided by 1-butanethiol and 1-butaneselenol, we conducted additional experiments (*vide infra*) to further establish these two molecules as new CTAs in mediating the DCT-controlled cationic polymerization of *p*MOS. For comparison, we also included 1-butanol in these experiments.

Kinetic studies can usually provide convincing evidence of controlled/living polymerization. For the kinetic study, the amount of TfOH was reduced to a concentration of 1 mmol to slow the propagation by reducing the concentration of active cationic chain ends, whereas all other polymerization conditions were kept constant as those used in previous experiments in this work (see the Experimental Section for details). Results from the kinetics study show that the experimental molar mass from the polymerizations mediated by 1-butanol has a relatively large deviation from the tabulated theoretical molar mass (Figure 1G, bottom). Consistent with our previous results,[10] an induction period was observed in the polymerization when using 1-butanol as the CTA (Figure 1D); in contrast, 1-butanethio- mediated polymerization shows pseudo-first-order kinetics (Figure 1E) and linear molar mass evolution (Figure 1G, bottom). That said, the experimental molar mass shows a slight deviation from the calculated molar mass. As the best nucleophile in this series, 1-butaneselenol-mediated polymerization shows pseudo-first-order kinetics (Figure 1F), a linear molar mass evolution (Figure 1G, bottom), and a low dispersity (Figure 1G, top). Notably, the experimental molar mass obtained from the 1-butaneselenol-controlled polymerization clearly shows the best agreement with the theoretical molar mass (Figure 1G, bottom). Also notable, the polymerization mediated by 1-butaneselenol took 50 min to reach high conversion (Figure 1F); in contrast, much less time was needed to reach similar conversions for the polymerizations mediated by 1-butanethiol (10 min) and 1-butanol (5 min). In fact, the longer polymerization time observed in the case of 1-butaneselenol is indicative of an increased number of chain-transfer events occurring to retard the rate of polymerization, which is consistent with the expected effect of the increased CTA nucleophilicity.[45,46]

To further investigate the importance of nucleophilicity of the CTA in the cationic polymerization of *p*MOS, we computed the Gibbs free energy values for the main equilibrium between the dormant species/propagating chain end and the chain-transfer intermediate (Figure 2A). For simplicity, we only chose one molecule of *p*MOS as the propagating chain end and one molecule of *p*MOS-CTA as the dormant chain in constructing the main equilibrium, and the transition state is simulated in Figure 2B. The computed Gibbs free energy values (Figure 2C) become more negative going down group 16 (O > S > Se), indicating increased likelihood of chain-transfer events which is consistent with the retardation observed.

Another key piece of evidence for a controlled/living polymerization is the chain extension. Thus, we lastly chose

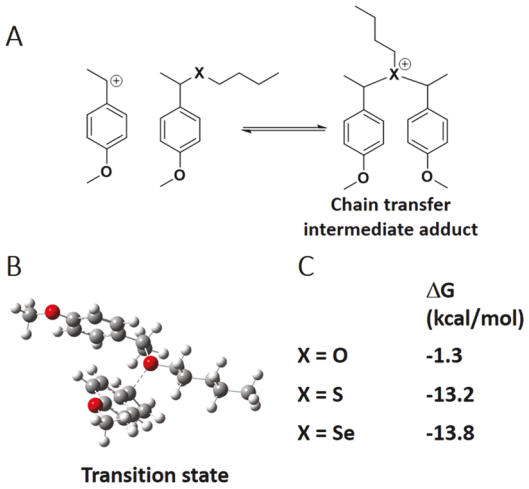

Figure 2. Models computed to simulate change in Gibbs free energy (A), transition state simulated to form the chain transfer intermediate adduct (B) and the resulting change of Gibbs free energy for 1-butanol, 1-butanethiol, and 1-butaneselenol (C).

to conduct a chain extension study, to demonstrate that a living chain end was indeed present and to show the potential utility of the cationic DCT-controlled polymerization. Experimentally, an in situ chain extension study was conducted with the nucleophilic aliphatic CTAs. The polymerization mediated by 1-butanol showed little ability for chain extension (from $M_{n,sec}$ = 4500 g mol^{-1}, $Đ$ = 1.36 to $M_{n,sec}$ = 5400 g mol^{-1}, $Đ$ = 1.35, Figure 3A). On the other hand, the polymerization

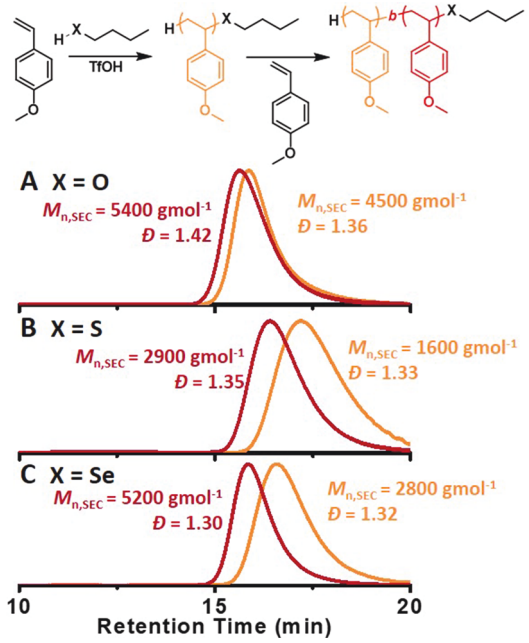

Figure 3. In situ chain extension study of nucleophilic aliphatic CTA in the polymerization of *p*MOS.

mediated by 1-butanethiol showed a clear chain extension (Figure 3B) coupled with a significant shift in molar mass (from $M_{n,sec}$ = 1600 g mol^{-1}, $Đ$ = 1.33 to $M_{n,sec}$ = 2900 g mol^{-1}, $Đ$ = 1.35). Finally, the polymerization controlled by 1-butaneselenol showed both a clear chain extension (Figure 3C) and respectable control over the molar mass (from $M_{n,sec}$ = 2800 g mol^{-1}, $Đ$ = 1.32 to $M_{n,sec}$ = 5200 g mol^{-1}, $Đ$ = 1.30),

https://dx.doi.org/10.1021/acs.macromol.0c00290
Macromolecules 2020, 53, 4303−4311

further demonstrating the controlled cationic DCT polymerization of *p*MOS by this unique CTA.

4. CONCLUSIONS

Though both can be polymerized cationically via a DCT-type mechanism, VEs (e.g., IBVE) and electron-rich styrenics (e.g., *p*MOS) are inherently different because of the difference in stability of the propagating carbocation. This inherent difference in the stability of propagating carbocations between VE and *p*MOS explains why weakly nucleophilic CTAs, such as weak acids, can provide control for the cationic polymerization of VEs but not for *p*MOS, as the latter requires more strongly nucleophilic CTA to attack the aromatically stabilized propagating carbocation of *p*MOS. Based on this reasoning, we hypothesize that the electronic structure of the propagating carbocation dictates the characteristics a CTA necessary to control the polymerization of a given monomer in a cationic process. We demonstrated, experimentally and computationally, that a better control of the cationic DCT polymerization can be achieved by increasing the nucleophilicity of CTA via promoting cationic chain-transfer events. Softness and hardness of the nucleophilic element are likely to play a role in the degenerative process as well because the nucleophile becomes softer going down group 16 (O, S and Se), which is consistent with a faster reaction of the soft nucleophile with a soft (delocalized) electrophilic cation. Furthermore, consistent with our findings, we discovered two novel selenium-based CTAs for the cationic DCT polymerization of *p*MOS, 1-benzeneselenol and 1-butaneselenol, both of which offer excellent control over molar mass and dispersity. Further investigation with other electron rich styrenic monomers will help expand the monomer scope of DCT-controlled cationic polymerization.

■ ASSOCIATED CONTENT

Supporting Information

The Supporting Information is available free of charge at https://pubs.acs.org/doi/10.1021/acs.macromol.0c00290.

SEC chromatogram, computational model of phenol and 4-cyanophenol, and ^{1}H-NMR-spectrum and MALDI-ToF mass spectra (PDF)

■ AUTHOR INFORMATION

Corresponding Authors

Joji Tanaka − *Department of Chemistry, University of North Carolina at Chapel Hill, Chapel Hill, North Carolina 27599, United States;* orcid.org/0000-0002-2134-8079; Email: joji@email.unc.edu

Wei You − *Department of Chemistry, University of North Carolina at Chapel Hill, Chapel Hill, North Carolina 27599, United States;* orcid.org/0000-0003-0354-1948; Email: wyou@unc.edu

Authors

Parker Thomas Boeck − *Department of Chemistry, University of North Carolina at Chapel Hill, Chapel Hill, North Carolina 27599, United States*

Shubin Liu − *Research Computing Center, University of North Carolina at Chapel Hill, Chapel Hill, North Carolina 27599, United States;* orcid.org/0000-0001-9331-0427

Complete contact information is available at: https://pubs.acs.org/10.1021/acs.macromol.0c00290

Author Contributions

The paper was written through contributions of all the authors. All the authors have given approval to the final version of the paper.

Funding

National Science Foundation (NSF) under the award CHE-1808055.

Notes

The authors declare no competing financial interest.

■ ACKNOWLEDGMENTS

P.T.B., J.T.,, and W.Y. were supported by the National Science Foundation under Award CHE-1808055. The authors acknowledge Dr. Marc A. ter Horst for NMR characterization, Alex Prevatte and Kyle Cushman for MALDI-ToF Characterization, Sally Lewis and Dr. Aaron Teator for help with THF-SEC characterization, and Professor Frank Leibfarth and Travis Varner for valuable tips on cationic polymerizations.

■ ABBREVIATIONS

CTA, chain-transfer agent; DCT, degenerative chain transfer; IBVE, isobutyl vinyl ether; MALDI-ToF, matrix-assisted laser desorption/ionization time of flight; NMR, nuclear magnetic resonance; RAFT, reversible addition−fragmentation chain transfer; SEC, size exclusion chromatography

■ REFERENCES

(1) Szwarc, M.; Levy, M.; Milkovich, R. Polymerization Initiated by Electron Transfer to Monomer. a New Method of Formation of Block Polymers1. *J. Am. Chem. Soc.* **1956**, *78*, 2656−2657.

(2) Miyamoto, M.; Sawamoto, M.; Higashimura, T. Living polymerization of isobutyl vinyl ether with hydrogen iodide/iodine initiating system. *Macromolecules* **1984**, *17*, 265−268.

(3) Webster, O. W.; Hertler, W. R.; Sogah, D. Y.; Farnham, W. B.; RajanBabu, T. V. Group-transfer polymerization. 1. A new concept for addition polymerization with organosilicon initiators. *J. Am. Chem. Soc.* **1983**, *105*, 5706−5708.

(4) Chiefari, J.; Chong, Y. K.; Ercole, F.; Krstina, J.; Jeffery, J.; Le, T. P. T.; Mayadunne, R. T. A.; Meijs, G. F.; Moad, C. L.; Moad, G.; Rizzardo, E.; Thang, S. H. Living Free-Radical Polymerization by Reversible Addition−Fragmentation Chain Transfer: The RAFT Process. *Macromolecules* **1998**, *31*, 5559−5562.

(5) Wang, J.-S.; Matyjaszewski, K. Controlled/"living" radical polymerization. atom transfer radical polymerization in the presence of transition-metal complexes. *J. Am. Chem. Soc.* **1995**, *117*, 5614−5615.

(6) Georges, M. K.; Veregin, R. P. N.; Kazmaier, P. M.; Hamer, G. K. Narrow molecular weight resins by a free-radical polymerization process. *Macromolecules* **1993**, *26*, 2987−2988.

(7) Kato, M.; Kamigaito, M.; Sawamoto, M.; Higashimura, T. Polymerization of Methyl Methacrylate with the Carbon Tetrachloride/Dichlorotris- (triphenylphosphine)ruthenium(II)/Methylaluminum Bis(2,6-di-tert-butylphenoxide) Initiating System: Possibility of Living Radical Polymerization. *Macromolecules* **1995**, *28*, 1721−1723.

(8) Aoshima, S.; Kanaoka, S. A Renaissance in Living Cationic Polymerization. *Chem. Rev.* **2009**, *109*, 5245−5287.

(9) Uchiyama, M.; Sakaguchi, M.; Satoh, K.; Kamigaito, M. A User-friendly Living Cationic Polymerization: Degenerative Chain-transfer Polymerization of Vinyl Ethers by Simply Using Mixtures of Weak and Superstrong Protonic Acids. *Chin. J. Polym. Sci.* **2019**, *37*, 851−857.

(10) Prasher, A.; Hu, H.; Tanaka, J.; Nicewicz, D. A.; You, W. Alcohol mediated degenerate chain transfer controlled cationic polymerisation of para-alkoxystyrene. *Polym. Chem.* **2019**, *10*, 4126−4133.

(11) Guerre, M.; Uchiyama, M.; Folgado, E.; Semsarilar, M.; Améduri, B.; Satoh, K.; Kamigaito, M.; Ladmiral, V. Combination of Cationic and Radical RAFT Polymerizations: A Versatile Route to Well-Defined Poly(ethyl vinyl ether)-block-poly(vinylidene fluoride) Block Copolymers. *ACS Macro Lett.* **2017**, *6*, 393−398.
(12) Kottisch, V.; Michaudel, Q.; Fors, B. P. Photocontrolled Interconversion of Cationic and Radical Polymerizations. *J. Am. Chem. Soc.* **2017**, *139*, 10665−10668.
(13) Peterson, B. M.; Kottisch, V.; Supej, M. J.; Fors, B. P. On Demand Switching of Polymerization Mechanism and Monomer Selectivity with Orthogonal Stimuli. *ACS Cent. Sci.* **2018**, *4*, 1228−1234.
(14) Satoh, K.; Fujiki, Y.; Uchiyama, M.; Kamigaito, M., Vinyl Ether/Vinyl Ester Copolymerization by Cationic and Radical Interconvertible Simultaneous Polymerization. *Reversible Deactivation Radical Polymerization: Mechanisms and Synthetic Methodologies*; American Chemical Society, 2018; Vol. *1284*, pp 323−334.
(15) Satoh, K.; Hashimoto, H.; Kumagai, S.; Aoshima, H.; Uchiyama, M.; Ishibashi, R.; Fujiki, Y.; Kamigaito, M. One-shot controlled/living copolymerization for various comonomer sequence distributions via dual radical and cationic active species from RAFT terminals. *Polym. Chem.* **2017**, *8*, 5002−5011.
(16) Aoshima, H.; Uchiyama, M.; Satoh, K.; Kamigaito, M. Interconvertible Living Radical and Cationic Polymerization through Reversible Activation of Dormant Species with Dual Activity. *Angew. Chem., Int. Ed.* **2014**, *53*, 10932−10936.
(17) Kottisch, V.; Supej, M. J.; Fors, B. P. Enhancing Temporal Control and Enabling Chain-End Modification in Photoregulated Cationic Polymerizations by Using Iridium-Based Catalysts. *Angew. Chem., Int. Ed.* **2018**, *57*, 8260−8264.
(18) Kottisch, V.; Michaudel, Q.; Fors, B. P. Cationic Polymerization of Vinyl Ethers Controlled by Visible Light. *J. Am. Chem. Soc.* **2016**, *138*, 15535−15538.
(19) Takeshima, H.; Satoh, K.; Kamigaito, M. R-Cl/SnCl4/n-Bu4NCl-induced direct living cationic polymerization of naturally-derived unprotected 4-vinylphenol, 4-vinylguaiacol, and 4-vinylcatechol in CH3CN. *Polym. Chem.* **2019**, *10*, 1192−1201.
(20) Takeshima, H.; Satoh, K.; Kamigaito, M. Naturally-Derived Amphiphilic Polystyrenes Prepared by Aqueous Controlled/Living Cationic Polymerization and Copolymerization of Vinylguaiacol with R-OH/BF3·OEt2. *Polymers* **2018**, *10*, 1404.
(21) Satoh, K.; Nakahara, A.; Mukunoki, K.; Sugiyama, H.; Saito, H.; Kamigaito, M. Sustainable cycloolefin polymer from pine tree oil for optoelectronics material: living cationic polymerization of β-pinene and catalytic hydrogenation of high-molecular-weight hydrogenated poly(β-pinene). *Polym. Chem.* **2014**, *5*, 3222−3230.
(22) Satoh, K. Controlled/living polymerization of renewable vinyl monomers into bio-based polymers. *Polym. J.* **2015**, *47*, 527−536.
(23) Hayashi, K.; Kanazawa, A.; Aoshima, S. Exceptional copolymerizability of o-phthalaldehyde in cationic copolymerization with vinyl monomers. *Polym. Chem.* **2019**, *10*, 3712−3717.
(24) Engler, A.; Phillips, O.; Miller, R. C.; Tobin, C.; Kohl, P. A. Cationic Copolymerization of o-Phthalaldehyde and Functional Aliphatic Aldehydes. *Macromolecules* **2019**, *52*, 4020−4029.
(25) Kawamura, M.; Kanazawa, A.; Kanaoka, S.; Aoshima, S. Sequence-controlled degradable polymers by controlled cationic copolymerization of vinyl ethers and aldehydes: precise placement of cleavable units at predetermined positions. *Polym. Chem.* **2015**, *6*, 4102−4108.
(26) Mimura, M.; Kanazawa, A.; Aoshima, S. ABC Pseudo-Periodic Sequence Control by Cationic Orthogonal Terpolymerization of Vinyl Ether, Oxirane, and Ketone. *Macromolecules* **2019**, *52*, 7572−7583.
(27) Teator, A. J.; Leibfarth, F. A. Catalyst-controlled stereoselective cationic polymerization of vinyl ethers. *Science* **2019**, *363*, 1439−1443.
(28) Teator, A. J.; Varner, T. P.; Jacky, P. E.; Sheyko, K. A.; Leibfarth, F. A. Polar Thermoplastics with Tunable Physical Properties Enabled by the Stereoselective Copolymerization of Vinyl Ethers. *ACS Macro Lett.* **2019**, *8*, 1559−1563.
(29) Tanaka, J.; Häkkinen, S.; Boeck, P. T.; Cong, Y.; Perrier, S.; Sheiko, S. S.; You, W. Orthogonal Cationic and Radical RAFT Polymerizations to Prepare Bottlebrush Polymers. *Angew. Chem., Int. Ed.* **2020**, *59*, 7203−7208.
(30) Uchiyama, M.; Satoh, K.; McKenzie, T. G.; Fu, Q.; Qiao, G. G.; Kamigaito, M. Diverse approaches to star polymers via cationic and radical RAFT cross-linking reactions using mechanistic transformation. *Polym. Chem.* **2017**, *8*, 5972−5981.
(31) Li, J.; Kerr, A.; Häkkinen, S.; Floyd, T.; Zhang, M.; Pan, X.; Zhu, X.; Perrier, S.; Zhu, J. Manganese carbonyl induced cationic reversible addition-fragmentation chain transfer (C-RAFT) polymerization under visible light. *Polym. Chem.* **2020**, *11*, 2724−2731.
(32) Uchiyama, M.; Satoh, K.; Kamigaito, M. Diversifying Cationic RAFT Polymerization with Various Counteranions: Generation of Cationic Species from Organic Halides and Various Metal Salts. *ACS Macro Lett.* **2016**, *5*, 1157−1161.
(33) Kottisch, V.; O'Leary, J.; Michaudel, Q.; Stache, E. E.; Lambert, T. H.; Fors, B. P. Controlled Cationic Polymerization: Single-Component Initiation under Ambient Conditions. *J. Am. Chem. Soc.* **2019**, *141*, 10605−10609.
(34) Kamigaito, M.; Maeda, Y.; Sawamoto, M.; Higashimura, T. Living cationic polymerization of isobutyl vinyl ether by hydrogen chloride/Lewis acid initiating systems in the presence of salts: in-situ direct NMR analysis of the growing species. *Macromolecules* **1993**, *26*, 1643−1649.
(35) Kumagai, S.; Nagai, K.; Satoh, K.; Kamigaito, M. In-Situ Direct Mechanistic Transformation from RAFT to Living Cationic Polymerization for (Meth)acrylate−Vinyl Ether Block Copolymers. *Macromolecules* **2010**, *43*, 7523−7531.
(36) Uchiyama, M.; Satoh, K.; Kamigaito, M. Cationic RAFT Polymerization Using ppm Concentrations of Organic Acid. *Angew. Chem., Int. Ed.* **2015**, *54*, 1924−1928.
(37) Perkowski, A. J.; You, W.; Nicewicz, D. A. Visible Light Photoinitiated Metal-Free Living Cationic Polymerization of 4-Methoxystyrene. *J. Am. Chem. Soc.* **2015**, *137*, 7580−7583.
(38) Uchiyama, M.; Satoh, K.; Kamigaito, M. Thioether-Mediated Degenerative Chain-Transfer Cationic Polymerization: A Simple Metal-Free System for Living Cationic Polymerization. *Macromolecules* **2015**, *48*, 5533−5542.
(39) Masuda, T. Structure and reactivity of vinyl ethers and styrene derivatives in cationic polymerization. *J. Polym. Sci. Polym. Chem. Ed.* **1973**, *11*, 2713−2717.
(40) Herzog, U. Synthesis and NMR Investigation of Selenobutyl Substituted Silanes and Oligosilanes. *J. Prakt. Chem.* **2000**, *342*, 379−388.
(41) Uchiyama, M.; Satoh, K.; Kamigaito, M. A phosphonium intermediate for cationic RAFT polymerization. *Polym. Chem.* **2016**, *7*, 1387−1396.
(42) Michaudel, Q.; Chauviré, T.; Kottisch, V.; Supej, M. J.; Stawiasz, K. J.; Shen, L.; Zipfel, W. R.; Abruña, H. D.; Freed, J. H.; Fors, B. P. Mechanistic Insight into the Photocontrolled Cationic Polymerization of Vinyl Ethers. *J. Am. Chem. Soc.* **2017**, *139*, 15530−15538.
(43) Uggerud, E. Nucleophilicity-Periodic Trends and Connection to Basicity. *Chem. Eur. J.* **2006**, *12*, 1127−1136.
(44) Yamada, S. Cation−π Interactions in Organic Synthesis. *Chem. Rev.* **2018**, *118*, 11353−11432.
(45) Moad, G.; Chiefari, J.; Chong, Y. K.; Krstina, J.; Mayadunne, R. T. A.; Postma, A.; Rizzardo, E.; Thang, S. H. Living free radical polymerization with reversible addition - fragmentation chain transfer (the life of RAFT). *Polym. Int.* **2000**, *49*, 993−1001.
(46) Moad, G. Mechanism and Kinetics of Dithiobenzoate-Mediated RAFT Polymerization - Status of the Dilemma. *Macromol. Chem. Phys.* **2014**, *215*, 9−26.

https://dx.doi.org/10.1021/acs.macromol.0c00290
Macromolecules 2020, 53, 4303−4311